Title
X-ray Absorption Spectra of Dissolved Polysulfides in Lithium–Sulfur Batteries from First-Principles

Journal
The Journal of Physical Chemistry Letters, 5(9)

ISSN
1948-7185

Authors
Pascal, Tod A
Wujcik, Kevin H
Velasco-Velez, Juan
et al.

Publication Date
2014-05-01

DOI
10.1021/jz500260s

Peer reviewed

THE JOURNAL OF PHYSICAL CHEMISTRY Letters

Letter

pubs.acs.org/JPCL

X-ray Absorption Spectra of Dissolved Polysulfides in Lithium–Sulfur Batteries from First-Principles

Tod A. Pascal,*[,†] Kevin H. Wujcik,[‡,§] Juan Velasco-Velez,[¶] Chenghao Wu,[¶] Alexander A. Teran,[‡,§] Mukes Kapilashrami,[∥] Jordi Cabana,[§,⊥] Jinghua Guo,[∥] Miquel Salmeron,[¶,□] Nitash Balsara,[‡,§] and David Prendergast*[,†]

[†]The Molecular Foundry, [¶]Material Science Division, [§]Environmental Energy Technologies Division, and [∥]Advanced Light Source, Lawrence Berkeley National Laboratory, Berkeley, California 94720, United States

[‡]Department of Chemical and Biomolecular Engineering and [□]Department of Materials Science and Engineering, University of California, Berkeley, California 94720, United States

[⊥]Department of Chemistry, University of Illinois at Chicago, Chicago, Illinois 60607, United States

Supporting Information

ABSTRACT: The X-ray absorption spectra (XAS) of lithium polysulfides (Li_2S_x) of various chain lengths (x) dissolved in a model solvent are obtained from first-principles calculations. The spectra exhibit two main absorption features near the sulfur K-edge, which are unambiguously interpreted as a pre-edge near 2471 eV due to the terminal sulfur atoms at either end of the linear polysulfide dianions and a main-edge near 2473 eV due to the (x − 2) internal atoms in the chain, except in the case of Li_2S_2, which only has a low-energy feature. We find an almost linear dependence between the ratio of the peaks and chain length, although the linear dependence is modified by the delocalized, molecular nature of the core-excited states that can span up to six neighboring sulfur atoms. Thus, our results indicate that the ratio of the peak area, and not the peak intensities, should be used when attempting to differentiate the polysulfides from XAS.

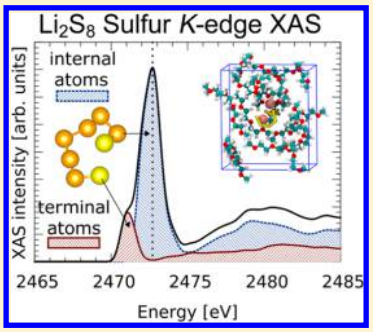

SECTION: Spectroscopy, Photochemistry, and Excited States

There has been significant interest recently in lithium sulfur batteries because, with a theoretical capacity of 1642 mA h/g and a specific energy of 2600 W h/kg,[1] these cells already satisfy the energy requirement of the 2020 U.S. DOE goals for transportation.[2] However, large-scale adoption of this technology has been hampered by numerous shortcomings, in particular, poor utilization of the active cathode material and rapid capacity fading during cycling.[3−5] Despite intense effort, the fundamental mechanisms underlying the operation of these batteries are still not well understood. What is known is that at the cathode, elemental sulfur (crystalline α-S_8) is reduced to lithium sulfide (Li_2S) according to the following, straightforward reaction: $S_8 + 16Li^+ + 16e^- \rightarrow 8Li_2S$. In reality, the cathode reaction is far more complex[6] and possibly proceeds through a series of stepwise redox reactions and competing disproportionation,[7−9] forming various lithium polysulfide intermediates[10,11] (Li_2S_x; x = 2−8) with progressively shorter linear sulfur chains until Li_2S is formed.[12] These polysulfides are believed to be soluble in the electrolyte, migrating away from the cathode during cycling, thereby resulting in irreversible loss of active material[13] and competing reactions at the unprotected anode surface.

Design principles for overcoming these limitations will undoubtedly require a molecular-level understanding of the solution-phase chemistries and their evolution under applied voltage. In particular, questions such as the reversibility of linear polysulfide formation from cyclic elemental sulfur and the chemical nature of the polysulfide species at a given state of charge need to be addressed. Answers to these questions hinge on the ability to identify the different polysulfides, and their relative amounts, in working cells.

With the aim of determining polysulfide speciation in working lithium sulfur cells or prepared Li–S mixtures, various nondestructive characterization techniques have been applied, including UV–vis,[8,9] Raman,[14] and NMR[8,15] spectroscopy, HPLC and EPR,[8] and X-ray diffraction.[16,17] Here, we focus on a powerful complementary technique, X-ray absorption spectroscopy (XAS), which provides an element-specific probe of local electronic structure that can be interpreted near the absorption onset (so-called near-edge fine structure) to indicate details of local chemistry, oxidation state, and/or atomic coordination. For example, a study at the sulfur K-edge (1s → 3p) attempted to quantify the effect of electrolyte solvent on polysulfide formation.[18] Another study at the carbon K-edge has been interpreted to indicate the incorporation of sulfur into a nanocomposite electrode material.[19] More recently, XAS at the S K-edge has been used to attempt to identify the polysulfide species formed during stages of electrochemical cycling.[15]

Received: February 5, 2014
Accepted: April 9, 2014
Published: April 9, 2014

   dx.doi.org/10.1021/jz500260s | J. Phys. Chem. Lett. 2014, 5, 1547−1551

Underlying these experimental studies are the general assumptions that canonical mixtures for a given ratio of Li/S leads to pure molecular phases in solution and that plateaus in cyclic voltammetry are indicative of the formation of soluble molecular species, Li_2S_x, which migrate away from the cathode.

Interpretation of experimental XAS is commonly achieved by fingerprinting, that is, comparison to known standards or their linear superposition. To date, there have been relatively few XAS studies of lithium polysulfides[15,18,20] and no published spectra of either pure or dissolved lithium polysulfides. As a result, fingerprinting has been attempted using solid standards[18,20] or sodium-substituted analogues.[15] By contrast, in this work, we directly simulate the XAS of lithium polysulfides dissolved in tetraglyme (tetraethylene glycol dimethyl ether, TEGDME) using first-principles molecular dynamics (FPMD) and spectral simulations, offering clear interpretation of the spectral features. Our goal is to determine the nature of the electronic transitions that underlie the XAS spectra of lithium polysulfides and thereby to assess the feasibility of XAS to detect and differentiate between polysulfide chains of various lengths.

Figure 1 shows the first-principles simulations of the sulfur K-edge XAS of dissolved lithium polysulfides (see inset) with chain lengths varying from 2 to 8. Generally, the spectra can be characterized by two peaks, a strong absorption feature between 2472.6 and 2473.9 eV (hereby denoted the main-edge), which is reminiscent of the so-called "white line" peak of elemental sulfur at 2472.6 eV (Figure S1a of the Supporting Information), and another feature between 2470.6 and 2471.5 eV (denoted the pre-edge). The only exception is di-lithium persulfide (Li_2S_2), which is characterized by a single feature at 2471.3 eV, lacking a main-edge peak (Table 1). The relative main/pre-edge peak splitting of 1−2 eV is in good agreement with experimental measurements on lithium polysulfide samples.[15,18]

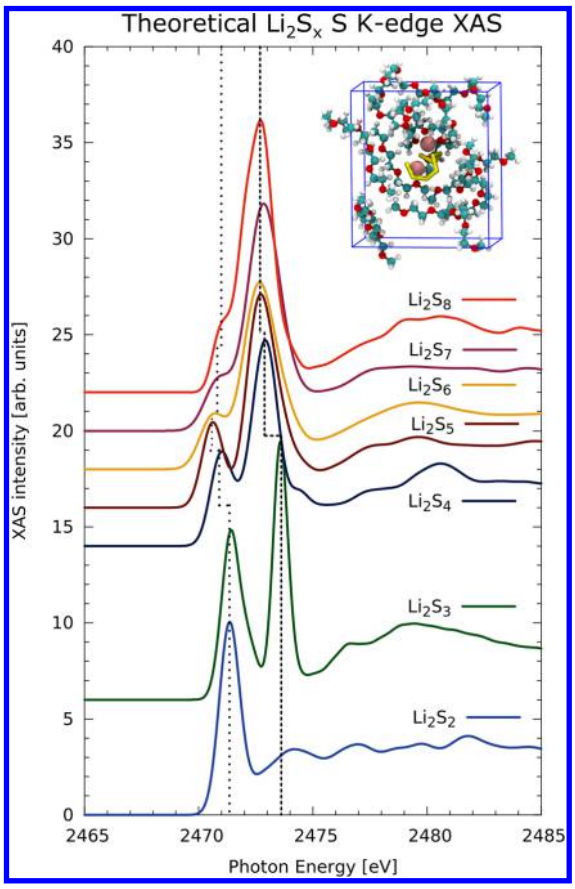

Figure 1. First-principles simulation of the sulfur K-edge XAS spectra of Li_2S_x dissolved in TEGDME (x = 2−8) obtained from XCH-DFT calculations of snapshots sampled from a 298 K FPMD simulation. The position of the pre-edge (black dotted vertical line) and main-edge (dashed vertical line) are shown to guide the eyes. (Inset) Representative snapshot of our FPMD simulation of a Li_2S_8 molecule with 10 TEGDME molecules. The sulfur (yellow spheres), lithium (pink), oxygen (red), carbon (green), and hydrogen (silver) atoms of TEGDME are shown.

Table 1. Average Sulfur K-Edge XAS Peak Position and Peak Intensities of Li_2S_x dissolved in TEGDME Determined from First-Principles Analysis[a]

	peak positions [eV]		normalized intensity [arb. units]		
Li_2S_x	pre	main	pre	main	main/pre area ratio
2	2471.3 (0.6)		18.9		
3	2471.5 (0.7)	2473.6 (0.4)	16.8	26.4	1.1
4	2471.0 (0.7)	2472.9 (0.8)	10.0	21.1	2.6
5	2470.6 (0.5)	2472.8 (1.0)	9.4	20.9	4.3
6	2470.5 (0.6)	2472.7 (1.1)	5.1	19.1	6.3
7	2470.8 (0.6)	2472.9 (1.0)	4.9	23.4	8.2
8	2471.0 (0.6)	2472.6 (1.0)	5.3	28.0	9.3

[a]The number in brackets represents the standard deviation (1σ).

Our calculations indicate that the main- and pre-edge XAS features arise from differently coordinated sulfur atoms in the same molecule. Consider Li_2S_8, with a linear polysulfide dianion composed of two terminal and six internal atoms. Schematically, S_8^{2-} is often represented with a formal charge of $1e^-$ associated with each of the terminal (dangling) sulfur atoms, with the internal atoms uncharged. Our density functional theory (DFT) calculations indicate that, while the terminal atoms do indeed have increased charge (i.e., increased local valence electron density) compared to the internal atoms, the charge is less than $1e^-$ (Figure S2, Supporting Information) due to hybridization of the molecular orbitals. Additionally, we also observe some charge transfer from the TEGDME solvent to the lithium polysulfide molecules, except for the Li_2S_2 and Li_2S_8 molecules, which are found to donate a small amount of charge to the solvent (Table S1 of the Supporting Information). The increased electronic charge at the terminal sulfur atoms leads to a reduced binding energy of the 1s core−electrons, and as reactive sites, we would also expect the lowest unoccupied molecular orbitals to be localized on these atoms. Both of these factors conspire to red shift the absorption onset of the terminal atoms with respect to those internal in the polysulfide chains. Specifically, for Li_2S_8, we observe that the pre-edge arises solely from the terminal atoms and sits 1.5 eV below the main-edge, to which only the internal atoms contribute (Figure 2). The XAS of the terminal sulfur atoms alone greatly resembles that of Li_2S_2, which is composed entirely of terminal atoms, while the internal sulfur atoms have a spectrum that is reminiscent of elemental sulfur (S_8), whose cyclic molecules have no termini.

We find that there is a linear correlation between the terminal/internal atom peak splitting and the associated partial atomic charge difference. Thus, the more distributed charges in

dx.doi.org/10.1021/jz500260s | J. Phys. Chem. Lett. 2014, 5, 1547−1551

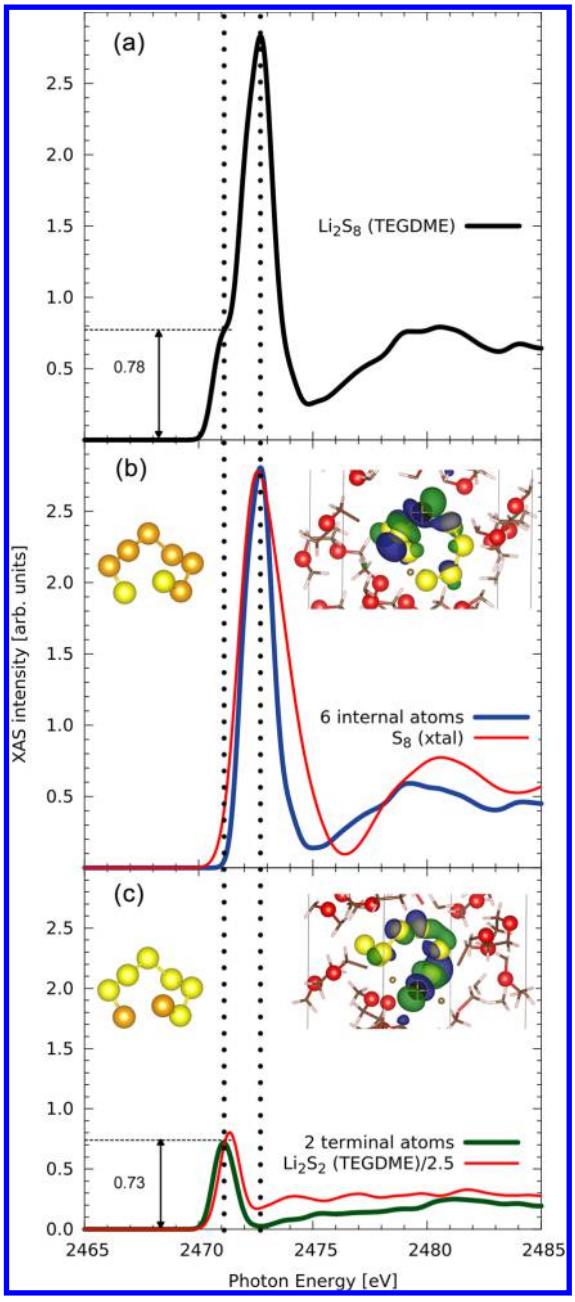

Figure 2. Sulfur K-edge XAS of Li_2S_8 dissolved in TEGDME. The dotted vertical lines indicate the position of the peak maxima and are presented to guide the eye. (a) Full spectrum including contributions from all eight sulfur atoms. The intensity of the pre-edge feature is indicated. (b) Spectral contribution of the six internal sulfur atoms (blue line) and comparison with XAS of elemental α-S_8 (dashed red line). (Left inset) Schematic of the S_8^{2-} molecule showing the six internal atoms in orange and the two terminal atoms in yellow. (Right inset) Representative electron density of the resulting 1s → 3p excited state for the internal sulfur atoms (yellow spheres). We adopt the convention that the positive phase of the density is colored green while the negative phase is colored blue. The carbon (gray), oxygen (red), and hydrogen (silver) TEGDME atoms near the Li_2S_8 molecule are shown. The lithium atoms (olive spheres) are also shown. The excited sulfur atom is indicated by the crossed sphere. (c) The spectral contribution of the two terminal atoms (as denoted by the left inset, green line) compared to the XAS of Li_2S_2 solvated in TEGDME (reduced by a factor of 2.5) is shown for comparison.

Li_2S_8 lead to a 1.5 eV peak splitting, which is visible as a shoulder in the XAS spectrum, while the more localized charges in Li_2S_3 result in a 2.1 eV peak splitting and two well-resolved peaks at 2471.7 and 2473.8 eV. On the basis of this interpretation, one would naturally expect the XAS of Li_2S_2 to present only one low-energy feature; the S_2^{2-} anion only has terminal atoms.

The electron density of the core-excited states of the dissolved lithium polysulfides is almost entirely confined to the sulfur molecule but delocalized along the chain (see right insets of Figure 2). This means that we can discuss changes in the XAS peak positions by only considering local S−S bond chemistry. Within this context, one might ask what are the factors that drive differences in the pre- and main-edge XAS features among the various polysulfides? Our calculations show a general red shift of the XAS peaks with increasing chain length, despite a calculated average decrease in the local valence electron density[21,22] on the sulfur atoms (Table S1, Supporting Information). We would rather expect a blue shift of the excitation energies arising from increased core-level binding due to reduced electronic screening[23] offered by a decrease in the local valence electron density around the excited sulfur atom. In competition with this effect, an increase in the average S−S bond length (as we observe in Figure S3 and Table S2, Supporting Information) would red shift peak positions due to a reduced splitting between bonding and antibonding valence molecular orbitals, resulting from reduced spatial overlap of atomic orbitals.[24] Specifically, in Li_2S_4 and Li_2S_5, the overall spectrum is red-shifted compared to Li_2S_3 because the decrease in the local valence electron density cannot compensate for the bond length increase. In contrast, when compared to Li_2S_2, the increased average S−S bond length in Li_2S_3 does not result in a red shift of the pre-edge peak position due to a relatively larger decrease in local valence electron density on the terminal S atoms, and ultimately the peak position remains unchanged. The peak positions of Li_2S_6, Li_2S_7, and Li_2S_8 are quite similar, as expected from the similarity of their local valence electron densities and S−S bond lengths.

Previously, the pre-edge feature in lithium polysulfide XAS has been interpreted as arising from transient, radical anions,[18] perhaps based on purported evidence of their formation (specifically $S_3^{\bullet-}$) from EPR measurements.[8] Of course, the inherently highly reactive, transient radicals would concurrently need to be long-lived and of an appreciable relative concentration in order to be visible to sulfur K-edge XAS. Instead, we propose a simpler explanation, that the spectral contributions of the terminal S atoms are the main contributors to the pre-edge. In another previous study, Kosugi et al.[25] performed ab initio calculations and temperature-dependent XAS measurements and showed that the spectrum of an isolated S_2 molecule has a low-energy 1s → π^* feature at 2469 eV, which is 2.5 eV lower in energy than the 1s → σ^* feature in both S_2 and S_8. The pre-edge feature in the Li_2S_x XAS spectrum has nothing to do with this transition because the π^* orbitals of the dianions are filled and inaccessible to excited electrons. The first available transition is to a σ^* orbital, which is significantly shifted to lower energies with respect to the neutral molecules by the increased electronic screening at the charged terminal sulfur atoms.

Our results also raise the possibility of distinguishing the polysulfides based on the main/pre-edge intensities.[15] One would expect the normalized intensity of the pre-edge feature to decrease with increasing chain length because the number of

dx.doi.org/10.1021/jz500260s | J. Phys. Chem. Lett. 2014, 5, 1547−1551

terminal sulfur atoms (2) remains constant while the number of internal sulfur atoms ($x - 2$) increases. Analysis of the intensity ratios suggests a fundamental difference in the polysulfides with $x \leq 4$ and $x > 4$ (Figure 3), which follow different linear trends.

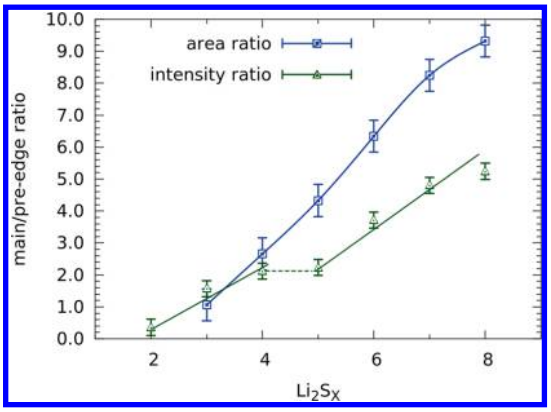

Figure 3. Plot of the main/pre-edge ratios versus x, the length of the Li_2S_x polysulfide chain. The pre- and main-edge features of the XAS from 2470 to 2475 eV are fit to a bimodal Gaussian function. The peak area ratio (blue squares) and intensity ratio (green triangles) are indicated. The lines are fits to the data (symbols) to guide the eye.

It is, perhaps, interesting to note that differentiation between soluble and insoluble polysulfides has been made at $x = 4$.[26] While conclusions can be made from peak intensities, we propose the ratio of peak areas (assuming Gaussian line shapes) as a better metric because bond length fluctuations at finite temperature can lead to enhanced spectral broadening and, therefore, less intense XAS features.[27] By employing peak areas, we incorporate the subtle finite temperature dependence, which we sample directly in our FPMD simulations. This analysis is also shown in Figure 3, where we find a monotonic increase in the main/pre-edge area ratio with increasing chain length, consistent with expectation. Li_2S_8 shows a slight deviation away from linearity, with a depressed main-edge intensity relative to that of the other polysulfides, a result that can be explained by considering the nature of the core-excited states that give rise to the XAS. As shown in the inset of Figure 2, these core-excited states are molecular in nature, that is, they delocalize across neighboring sulfur atoms, and initial analysis suggests that spatially, they span up to six atoms. Thus, in Li_2S_8, the core-excited states of the internal atoms span the entire molecule and are more delocalized than the terminal atoms, thereby decreasing the main-edge peak intensity relative to the pre-edge.

We conclude by noting that our simulated XAS avoids numerous ambiguities present in experiments, including the potential coexistence of multiple polysulfide species (not necessarily at chemical equilibrium) in ratios that are likely a complex function of experimental conditions and electrochemical state. These ambiguities further complicate attempts to draw conclusions on the nature of polysulfide speciation based solely on experimental peak ratios. We note that the role of changes in bond length and partial atomic charges in modifying XAS peak positions is a general phenomenon, and even though these effects are often overlooked in contemporary XAS literature, they can be powerful predictive tools, particularly when considering the effect of the atomic environment on measured XAS peak positions. Our future work will extend beyond pure phases in dilute solution and focus on quantifying the effect of the local polysulfide environment on X-ray absorption spectra.

COMPUTATIONAL METHODS

Theoretical methods of calculating XAS from first principles all involve approximations to Fermi's golden rule. In this study, we employ constrained-occupancy DFT calculations within the excited electron and core-hole (XCH) approach.[28] In brief, in XCH, the core-hole produced by the absorption of the X-ray photon is modeled in the presence of the associated excited electron, placed in the lowest available empty state of the system. The higher-energy excited states are approximated using the unoccupied portion of the Kohn−Sham DFT eigenspectrum, within the resulting XCH self-consistent field. Details of the computational procedure are presented in the Supporting Information. Other approaches for calculating XAS spectra are found in the literature, such as those based on time-dependent DFT or more computationally expensive calculations that explicitly account for the electron and core-hole interaction by solving the Bethe−Salpeter equation.[29−32] We find that our approach achieves a reasonable balance between the accuracy and efficiency needed to capture the physics in these finite-temperature solution-phase systems.

We are able to predict absolute peak positions through an energy alignment scheme based on formation energies and a single element-specific calibration, in this case matching the calculated XAS spectra of an isolated S_2 molecule to experiment.[25] In order to approximate the solution-phase reality of a typical experiment, the ensemble-averaged XAS samples an exploration of configuration space by a single polysulfide Li_2S_x complex solvated by TEGDME based on extracting snapshots from FPMD simulations[33,34] at a temperature of 298 K. This approach has been validated by comparison to high-resolution experimental XAS measurements in numerous previous studies.[27,35] We provide additional validating here by showing excellent agreement with experiment for elemental sulfur and lithium sulfide (Figure S1, Supporting Information).

ASSOCIATED CONTENT

Supporting Information

Detailed computational methods, data for XAS spectra, Figures S1−S3 and Tables S1 and S2, showing a comparison of the experimental and theoretical XAS of Li_2S and S_8, the partial molecular charges, and S−S bond length distribution on each Li_2S_x molecule from the first-principles molecular dynamics (FPMD) simulations. This material is available free of charge via the Internet at http://pubs.acs.org.

AUTHOR INFORMATION

Corresponding Authors

*E-mail: tapascal@lbl.gov (T.A.P.).
*E-mail: dgprendergast@lbl.gov (D.P.).

Notes

The authors declare no competing financial interest.

ACKNOWLEDGMENTS

This work was supported by the Assistant Secretary for Energy Efficiency and Renewable Energy, Office of Vehicle Technologies of the U.S. Department of Energy under Contract DE-AC02-05CH11231 under the Batteries for Advanced Transportation Technologies (BATT) Program and a Laboratory

Directed Research and Development grant at Lawrence Berkeley National Laboratory. Theory and simulations by T.A.P. and D.P. were performed as a user project at the Molecular Foundry, Lawrence Berkeley National Laboratory, supported by the Office of Science, Office of Basic Energy Sciences, of the U.S. Department of Energy under Contract No. DE-AC02-05CH11231. Spectral simulations used resources of the National Energy Research Scientific Computing Center, which is supported by the Office of Science of the U.S. Department of Energy under Contract No. DE-AC02-05CH11231. J.V.V. gratefully acknowledges financial support from the Alexander von Humboldt foundation.

REFERENCES

(1) Peramunage, D.; Licht, S. A Solid Sulfur Cathode for Aqueous Batteries. *Science* **1993**, *261*, 1029−1032.
(2) David, H.; Pat, D.; Dane, B.; Dave, D.; Linda, H.; John, V. *U.S. Department of Energy Vehicle Battery R&D: Current Scope and Future Directions*; U.S. Department of Energy: Washington, DC, 2012.
(3) Manthiram, A.; Fu, Y.; Su, Y.-S. Challenges and Prospects of Lithium−Sulfur Batteries. *Acc. Chem. Res.* **2012**, *46*, 1125−1134.
(4) Evers, S.; Nazar, L. F. New Approaches for High Energy Density Lithium−Sulfur Battery Cathodes. *Acc. Chem. Res.* **2012**, *46*, 1135−1143.
(5) Cheon, S. E.; Choi, S. S.; Han, J. S.; Choi, Y. S.; Jung, B. H.; Lim, H. S. Capacity Fading Mechanisms on Cycling a High-Capacity Secondary Sulfur Cathode. *J. Electrochem. Soc.* **2004**, *151*, A2067−A2073.
(6) Rauh, R. D.; Shuker, F. S.; Marston, J. M.; Brummer, S. B. Formation of Lithium Polysulfides in Aprotic Media. *J. Inorg. Nucl. Chem.* **1977**, *39*, 1761−1766.
(7) Yamin, H.; Gorenshtein, A.; Penciner, J.; Sternberg, Y.; Peled, E. Lithium Sulfur Battery Oxidation/Reduction Mechanisms of Polysulfides in Thf Solutions. *J. Electrochem. Soc.* **1988**, *135*, 1045−1048.
(8) Barchasz, C.; Molton, F.; Duboc, C.; Leprêtre, J.-C.; Patoux, S.; Alloin, F. Lithium/Sulfur Cell Discharge Mechanism: An Original Approach for Intermediate Species Identification. *Anal. Chem.* **2012**, *84*, 3973−3980.
(9) Patel, M. U.; Demir-Cakan, R.; Morcrette, M.; Tarascon, J. M.; Gaberscek, M.; Dominko, R. Li−S Battery Analyzed by UV/Vis in Operando Mode. *ChemSusChem* **2013**, *6*, 1177−1181.
(10) Akridge, J. R.; Mikhaylik, Y. V.; White, N. Li/S Fundamental Chemistry and Application to High-Performance Rechargeable Batteries. *Solid State Ionics* **2004**, *175*, 243−245.
(11) Kumaresan, K.; Mikhaylik, Y.; White, R. E. A Mathematical Model for a Lithium−Sulfur Cell. *J. Electrochem. Soc.* **2008**, *155*, A576−A582.
(12) Rauh, R. D.; Abraham, K. M.; Pearson, G. F.; Surprenant, J. K.; Brummer, S. B. Lithium-Dissolved Sulfur Battery with an Organic Electrolyte. *J. Electrochem. Soc.* **1979**, *126*, 523−527.
(13) Mikhaylik, Y. V.; Akridge, J. R. Polysulfide Shuttle Study in the Li/S Battery System. *J. Electrochem. Soc.* **2004**, *151*, A1969−A1976.
(14) Wang, H.; Yang, Y.; Liang, Y.; Robinson, J. T.; Li, Y.; Jackson, A.; Cui, Y.; Dai, H. Graphene-Wrapped Sulfur Particles as a Rechargeable Lithium−Sulfur Battery Cathode Material with High Capacity and Cycling Stability. *Nano Lett.* **2011**, *11*, 2644−2647.
(15) Cuisinier, M.; Cabelguen, P.-E.; Evers, S.; He, G.; Kolbeck, M.; Garsuch, A.; Bolin, T.; Balasubramanian, M.; Nazar, L. F. Sulfur Speciation in Li−S Batteries Determined by Operando X-ray Absorption Spectroscopy. *J. Phys. Chem. Lett.* **2013**, *4*, 3227−3232.
(16) Cheon, S.-E.; Ko, K.-S.; Cho, J.-H.; Kim, S.-W.; Chin, E.-Y.; Kim, H.-T. Rechargeable Lithium Sulfur Battery I. Structural Change of Sulfur Cathode During Discharge and Charge. *J. Electrochem. Soc.* **2003**, *150*, A796−A799.
(17) Nelson, J.; Misra, S.; Yang, Y.; Jackson, A.; Liu, Y.; Wang, H.; Dai, H.; Andrews, J. C.; Cui, Y.; Toney, M. F. In Operando X-ray Diffraction and Transmission X-ray Microscopy of Lithium Sulfur Batteries. *J. Am. Chem. Soc.* **2012**, *134*, 6337−6343.
(18) Gao, J.; Lowe, M. A.; Kiya, Y.; Abruna, H. D. Effects of Liquid Electrolytes on the Charge−Discharge Performance of Rechargeable Lithium/Sulfur Batteries: Electrochemical and In-Situ X-ray Absorption Spectroscopic Studies. *J. Phys. Chem. C* **2011**, *115*, 25132−25137.
(19) Ji, L.; Rao, M.; Zheng, H.; Zhang, L.; Li, Y.; Duan, W.; Guo, J.; Cairns, E. J.; Zhang, Y. Graphene Oxide as a Sulfur Immobilizer in High Performance Lithium/Sulfur Cells. *J. Am. Chem. Soc.* **2011**, *133*, 18522−18525.
(20) Patel, M. U. M.; Arčon, I.; Aquilanti, G.; Stievano, L.; Mali, G.; Dominko, R. X-ray Absorption Near-Edge Structure and Nuclear Magnetic Resonance Study of the Lithium−Sulfur Battery and Its Components. *ChemPhysChem* **2014**, In press.
(21) Henkelman, G.; Arnaldsson, A.; Jónsson, H. A Fast and Robust Algorithm for Bader Decomposition of Charge Density. *Comput. Mater. Sci.* **2006**, *36*, 354−360.
(22) Bader, R. F. *Atoms in Molecules*; Wiley Online Library: New York, 1990.
(23) LaVilla, R. E.; Deslattes, R. D. K-Absorption Fine Structures of Sulfur in Gaseous Sf. *J. Chem. Phys.* **1966**, *44*, 4399.
(24) Fukui, K.; Yonezawa, T.; Shingu, H. A Molecular Orbital Theory of Reactivity in Aromatic Hydrocarbons. *J. Chem. Phys.* **1952**, *20*, 722−725.
(25) Rühl, E.; Flesch, R.; Tappe, W.; Novikov, D.; Kosugi, N. Sulfur 1s Excitation of S2 and S8: Core−Valence- and Valence−Valence-Exchange Interaction and Geometry-Specific Transitions. *J. Chem. Phys.* **2002**, *116*, 3316−3322.
(26) Yamin, H.; Peled, E. Electrochemistry of a Nonaqueous Lithium/Sulfur Cell. *J. Power Sources* **1983**, *9*, 281−287.
(27) Pascal, T. A.; Boesenberg, U.; Kostecki, R.; Richardson, T. J.; Weng, T.-C.; Sokaras, D.; Nordlund, D.; McDermott, E.; Moewes, A.; Cabana, J.; Prendergast, D. Finite Temperature Effects on the X-ray Absorption Spectra of Lithium Compounds: First-Principles Interpretation of X-ray Raman Measurements. *J. Chem. Phys.* **2014**, *140*, 034107−034121.
(28) Prendergast, D.; Galli, G. X-ray Absorption Spectra of Water from First Principles Calculations. *Phys. Rev. Lett.* **2006**, *96*, 215502.
(29) Shirley, E. L. Ab Initio Inclusion of Electron−Hole Attraction: Application to X-ray Absorption and Resonant Inelastic X-ray Scattering. *Phys. Rev. Lett.* **1998**, *80*, 794−797.
(30) Shirley, E. L. Bethe−Salpeter Treatment of X-ray Absorption Including Core−Hole Multiplet Effects. *J. Electron Spectrosc. Relat. Phenom.* **2005**, *144*, 1187−1190.
(31) Olovsson, W.; Tanaka, I.; Puschnig, P.; Ambrosch-Draxl, C. Near-Edge Structures from First Principles All-Electron Bethe−Salpeter Equation Calculations. *J. Phys.: Condens. Matter* **2009**, *21*, 104205.
(32) Vinson, J.; Kas, J.; Vila, F.; Rehr, J.; Shirley, E. Theoretical Optical and X-ray Spectra of Liquid and Solid H_2O. *Phys. Rev. B* **2012**, *85*, 045101.
(33) VandeVondele, J.; Krack, M.; Mohamed, F.; Parrinello, M.; Chassaing, T.; Hutter, J. Quickstep: Fast and Accurate Density Functional Calculations Using a Mixed Gaussian and Plane Waves Approach. *Comput. Phys. Commun.* **2005**, *167*, 103−128.
(34) Lippert, G.; Hutter, J.; Parrinello, M. A Hybrid Gaussian and Plane Wave Density Functional Scheme. *Mol. Phys.* **1997**, *92*, 477−487.
(35) Drisdell, W. S.; Poloni, R.; McDonald, T. M.; Long, J. R.; Smit, B.; Neaton, J. B.; Prendergast, D.; Kortright, J. B. Probing Adsorption Interactions in Metal−Organic Frameworks Using X-ray Spectroscopy. *J. Am. Chem. Soc.* **2013**, *135*, 18183−18190.